# Seismic response of combined primary-secondary structures with the component-mode synthesis method

## Abstract

This paper deals with the dynamic analysis of primary-secondary combined systems. The problem of selecting the vibrational modes to be retained in analysis is first addressed, for the case of secondary substructures which may possess numerous low-frequency modes with negligible mass, and a dynamic mode acceleration method (DyMAM) is adopted in view of the application for seismic analysis. The influence of various approaches to build the viscous damping matrix of the primary-secondary assembly is then investigated, and a novel technique based on modal damping superposition is proposed. The results of a parametric study for a representative staircase system multi-connected to a two-dimensional multi-storey frame reveal that the DyMAM correction is capable of increasing the response accuracy with a reduced number of modes compared to the classical MAM (modal acceleration method). Furthermore, a new technique is proposed for assembling the damping matrix, which is shown to be a convenient alternative for modelling the dissipative forces in composite systems. Indeed, while mass and stiffness matrices can unambiguously be defined, various assumptions can be made for the damping matrix, inducing considerable variation in the predicted seismic response.

**Keywords:** dynamic analysis, modal analysis, nonstructural components, secondary substructures, seismic engineering, viscous damping.

# 1 Introduction

The seismic analysis and design of secondary attachments to buildings or industrial facilities is a topic of broad engineering interest, increasingly attracting the attention of researchers and practitioners. Examples of secondary subsystems include suspended

ceilings and non-structural walls, piping systems and antennas, storage tanks, electrical transformers and glass façades. Although not part of the load bearing structure, their significance stems from the survivability requirement in the aftermath of a seismic event and their vast contribution to the overall construction costs [1]. Nevertheless, past earthquakes have demonstrated that current methods for the seismic analysis of secondary substructures lack the necessary rigour and robustness, resulting in expensive and often unreliable solutions [2, 3, 4, 5].

Secondary subsystems can be highly sensitive to accelerations and inter-storey drifts, and their seismic performance is influenced by the primary-secondary dynamic interaction, which in many situations needs to be accounted for [6]. Additionally, when the analysis is carried out in conjunction with the supporting structure, the composite system will typically possess complex-valued eigenproperties, while the solution may be cumbersome and impractical. Addressing these limitations, the component-mode synthesis method (MSM) [7, 8], is an efficient computational strategy to handle the dynamic interaction between primary and secondary components under dynamic loads. The idea is to project the equations of motion on the reduced modal space, which is conveniently defined by the relevant modes of vibration of the primary structure and secondary attachment. Consequently, the response of the two components can simultaneously be evaluated with an acceptable computational time, without resorting to the combined structural model.

In the determination of the dynamic structural response of individual systems, mode superposition principles are exploited. As such, the mode displacement method (MDM) is typically employed, where the high-frequency modes are truncated, based on the assumption that their contribution is negligible beyond a certain threshold (e.g. when the cumulated participating modal mass exceeds 90% [9]). This may lead to large inaccuracies in the evaluation of displacements and their derivatives, increasing compexity and computational demand. To alleviate this, various modal correction techniques have been proposed in the literature, appending to the MDM solution a contribution accounting for the higher modes. In the well known mode acceleration method (MAM), for instance, and its variants [10, 11, 12, 13], a pseudo-static adjustment is used, under the assumption that inertial effects of the high-frequency modes are negligible, which however in some cases can lead to considerable errors. Notwithstanding such techniques have only been pursued to the case of individual subsystems, the MSM method motivates their applicability, to quantify their benefits, to the case of composite systems.

Complementing the aforementioned considerations, an intrinsic aspect related to the seismic response of secondary systems is the characterisation of dissipative forces, which has been an active research area in the field of linear structural dynamics. In the time-domain analysis, damping is typically idealised as viscous, due to the associated modelling simplifications and the difficulties in representing the actual mechanisms of energy dissipation. Two procedures are readily available for constructing a consistent damping matrix of individual systems based on estimation of modal damping ratios. If the system possesses classical normal modes (i.e. if and only if the Caughey

and O'Kelly condition is met [14]), a particular case of viscous damping, known as 'Rayleigh damping', can be assumed, expressing it as a linear combination of mass and stiffness. As a matter of fact, a more general form is available via a series expression the 'Caughey damping', in which Rayleigh is viewed as a special case. Lastly, a viable alternative is the superposition of the significant modal damping matrices [15].

Motivated by these considerations, this paper deals with the seismic response of coupled dynamic systems. Firstly, the selection of the modes of vibration to be retained in the analyses is discussed. While it is still doable to cumulate the mass of the first modes for the primary structure, until a certain threshold is reached, the same criterion can hardly be applied for secondary attachments, as they may possess numerous low-frequency modes with negligible mass. To overcome this problem, a convenient application of the dynamic MAM (DyMAM) [16] is proposed, to account for the contribution of the truncated modes of the secondary subsystem. Secondly, the influence of various approaches to construct the damping matrix of the primary-secondary assembly is investigated, and a novel technique based on the modal damping superposition is proposed. All the analyses are carried out on a staircase system multi-connected to a two-dimensional multi-storey frame, which further extends the results recently reported by Kasinos et al. [17] for single-degree-of-freedom secondary attachments. It is shown that the proposed DyMAM correction is capable of improving the truncation error due to the MDM while it concurrently corrects the discrepancy introduced by MAM, thus increasing the response accuracy. Furthermore, the proposed technique for assembling the damping matrix is shown to be a convenient alternative for modelling the dissipative forces in the composite system.

# 2 Combined system vibration via mode synthesis

## 2.1 Undamped motion

Let us consider the case of a S substructure with $n_{\mathrm{S}}$ degrees of freedom (DoFs) multiply attached to a P system with $n_{\mathrm{P}}$ DoFs. Within the linear-elastic range, the undamped seismic motion is governed by:

$$\mathbf{M} \cdot \ddot{\mathbf{u}}(t) + \mathbf{K} \cdot \mathbf{u}(t) = -\mathbf{M} \cdot \boldsymbol{\tau}\, \ddot{u}_g(t)\,, \tag{1}$$

where $\mathbf{u}\,(t) = \left\{ \mathbf{u}_{\mathrm{S}}^{\top}\,(t) \,\vdots\, \mathbf{u}_{\mathrm{P}}^{\top}\,(t) \right\}^{\top}$ is the partitioned array collecting the $n$ DoFs $(n = n_{\mathrm{S}} + n_{\mathrm{P}})$ of the combined dynamic system, in which $\mathbf{u}_{\mathrm{S}}\,(t) = \{u_{\mathrm{S},1}\,(t), \ldots, u_{\mathrm{S},n_{\mathrm{S}}}\,(t)\}^{\top}$ and $\mathbf{u}_{\mathrm{P}}\,(t) = \{u_{\mathrm{P},1}\,(t), \ldots, u_{\mathrm{P},n_{\mathrm{P}}}\,(t)\}^{\top}$ are arrays listing the DoFs of the S and P components, respectively, and the superscripted $\top$ is the transpose operator; $\boldsymbol{\tau} = \left\{ \boldsymbol{\tau}_{\mathrm{S}}^{\top} \,\vdots\, \boldsymbol{\tau}_{\mathrm{P}}^{\top} \right\}^{\top}$ is the partitioned array of seismic incidence; $\ddot{u}_g(t)$ is the ground acceleration; $\mathbf{M}$ and $\mathbf{K}$ are the matrices of mass and elastic stiffness, respectively, which can be partitioned

as:

$$\mathbf{M} = \left[\begin{array}{c:c} \mathbf{M}_{\mathrm{S}} & \mathbf{O}_{n_{\mathrm{S}} \times n_{\mathrm{P}}} \\ \hdashline \mathbf{O}_{n_{\mathrm{P}} \times n_{\mathrm{S}}} & \mathbf{M}_{\mathrm{P}} \end{array}\right] \; ; \quad \mathbf{K} = \left[\begin{array}{c:c} \mathbf{K}_{\mathrm{S}} & \mathbf{K}_{\mathrm{SP}} \\ \hdashline \mathbf{K}_{\mathrm{SP}}^{\top} & \mathbf{K}_{\mathrm{P}} + \mathbf{K}_{\mathrm{PP}} \end{array}\right] , \tag{2}$$

where $\{\mathbf{M}_{\mathrm{S}}, \mathbf{K}_{\mathrm{S}}\}$ and $\{\mathbf{M}_{\mathrm{P}}, \mathbf{K}_{\mathrm{P}}\}$ are the two pairs of mass and stiffness matrices of the S and P subsystems, individually considered, in which the P structure is assumed to be fixed to the ground, while the S subsystem is also fixed to the support points on P; and $\mathbf{O}_{r \times s}$ denotes a zero matrix with $r$ rows and $s$ columns. Furthermore, $\mathbf{K}_{\mathrm{SP}}$ is the stiffness matrix coupling P and S; $\mathbf{K}_{\mathrm{PP}}$ represents the additional stiffness in the P structure due to the presence of the S subsystem. The elements of both $\mathbf{K}_{\mathrm{SP}}$ and $\mathbf{K}_{\mathrm{PP}}$ only depend on the stiffness of the links used to connect P and S components.

The number of DoFs in the dynamic analysis can significantly be reduced by projecting the differential equations of motion onto the modal subspaces. This requires the following $n \times m$ transformation of coordinates:

$$\widetilde{\mathbf{u}}(t) = \mathbf{\Gamma} \cdot \mathbf{q}(t) \, , \tag{3}$$

in which $\mathbf{q}\,(t) = \left\{ \mathbf{q}_{\mathrm{S}}^{\top}\,(t) \,\middle|\, \mathbf{q}_{\mathrm{P}}^{\top}\,(t) \right\}^{\top}$ is the $m$-dimensional array $(m = m_{\mathrm{S}} + m_{\mathrm{P}})$ collecting the modal coordinates of the P-S system, where those of the S subsystem, listed in the array $\mathbf{q}_{\mathrm{S}}\,(t) = \{q_{\mathrm{S},1}\,(t), \ldots, q_{\mathrm{S},m_{\mathrm{S}}}\,(t)\}^{\top}$ precede those of the P structure, $\mathbf{q}_{\mathrm{P}}\,(t) = \{q_{\mathrm{P},1}\,(t), \ldots, q_{\mathrm{P},m_{\mathrm{P}}}\,(t)\}^{\top}$; and $\mathbf{\Gamma}$ is a transformation matrix, conveniently assembled as:

$$\mathbf{\Gamma} = \left[\begin{array}{c:c} \mathbf{\Phi}_{\mathrm{S}} & \mathbf{\Psi}_{\mathrm{SP}} \\ \hdashline \mathbf{O}_{n_{\mathrm{P}} \times m_{\mathrm{S}}} & \mathbf{\Phi}_{\mathrm{P}} \end{array}\right] , \tag{4}$$

where $\mathbf{\Phi}_{\mathrm{S}} = [\phi_{\mathrm{S},1} \ldots \phi_{\mathrm{S},m_{\mathrm{S}}}]$ and $\mathbf{\Phi}_{\mathrm{P}} = [\phi_{\mathrm{P},1} \ldots \phi_{\mathrm{P},m_{\mathrm{P}}}]$ are the $n_{\mathrm{S}} \times m_{\mathrm{S}}$ and $n_{\mathrm{P}} \times m_{\mathrm{P}}$ modal matrices for the S and P subsystems, respectively; and $\mathbf{\Psi}_{\mathrm{SP}} = [\psi_{\mathrm{SP},1} \ldots \psi_{\mathrm{SP},m_{\mathrm{S}}}]$ is the $n_{\mathrm{S}} \times m_{\mathrm{P}}$ coupling matrix.

The two modal matrices can be obtained by solving two independent real-valued eigenproblems, which neglect the interaction effects between the two subsystems [18]:

$$\mathbf{M}_{\mathrm{S}} \cdot \mathbf{\Phi}_{\mathrm{S}} \cdot \mathbf{\Omega}_{\mathrm{S}}^{2} = \mathbf{K}_{\mathrm{S}} \cdot \mathbf{\Phi}_{\mathrm{S}} \, ; \quad \mathbf{M}_{\mathrm{P}} \cdot \mathbf{\Phi}_{\mathrm{P}} \cdot \mathbf{\Omega}_{\mathrm{P}}^{2} = \mathbf{K}_{\mathrm{P}} \cdot \mathbf{\Phi}_{\mathrm{P}} \, , \tag{5}$$

with the ortho-normal condition $\mathbf{\Phi}_{\mathrm{S}}^{\top} \cdot \mathbf{M}_{\mathrm{S}} \cdot \mathbf{\Phi}_{\mathrm{S}} = \mathbf{I}_{m_{\mathrm{S}}}$ and $\mathbf{\Phi}_{\mathrm{P}}^{\top} \cdot \mathbf{M}_{\mathrm{P}} \cdot \mathbf{\Phi}_{\mathrm{P}} = \mathbf{I}_{m_{\mathrm{P}}}$. In Eqs. (5), $\mathbf{\Omega}_{\mathrm{S}}$ and $\mathbf{\Omega}_{\mathrm{P}}$ are the diagonal spectral matrices, listing the modal circular frequencies of S and P, respectively; and $\mathbf{I}_{r}$ stands for the identity matrix of size $r$.

The coupling matrix can be obtained as:

$$\mathbf{\Psi}_{\mathrm{SP}} = \mathbf{N}_{\mathrm{SP}} \cdot \mathbf{\Phi}_{\mathrm{P}} \, , \tag{6a}$$

where $\mathbf{N}_{\mathrm{SP}}$ is the matrix of pseudo-static influence of P on S, which can in turn be determined by solving the matrix equation:

$$\mathbf{K}_{\mathrm{S}} \cdot \mathbf{N}_{\mathrm{SP}} = -\mathbf{K}_{\mathrm{SP}} \,. \tag{6b}$$

Substituting Eq. (3) into Eq. (1), and premultiplying the result by $\mathbf{\Gamma}^{\top}$, the equation of motion in the modal subspaces is ruled by:

$$\mathbf{m} \cdot \ddot{\mathbf{q}}(t) + \mathbf{k} \cdot \mathbf{q}(t) = \mathbf{g}\, \ddot{u}_g(t) \,, \tag{7}$$

where $\mathbf{m}$ and $\mathbf{k}$ are the matrices of mass and stiffness, while $\mathbf{g}$ is the influence vector of seismic incidence in the reduced modal subspace:

$$\mathbf{m} = \mathbf{\Gamma}^{\top} \cdot \mathbf{M} \cdot \mathbf{\Gamma} = \left[\begin{array}{c:c} \mathbf{I}_{m_{\mathrm{S}}} & \mathbf{m}_{\mathrm{SP}} \\ \hdashline \mathbf{m}_{\mathrm{SP}}^{\top} & \mathbf{I}_{m_{\mathrm{P}}} + \mathbf{m}_{\mathrm{PP}} \end{array}\right] ; \tag{8a}$$

$$\mathbf{k} = \mathbf{\Gamma}^{\top} \cdot \mathbf{K} \cdot \mathbf{\Gamma} = \left[\begin{array}{c:c} \mathbf{\Omega}_{\mathrm{S}}^2 & \mathbf{O}_{m_{\mathrm{S}} \times m_{\mathrm{P}}} \\ \hdashline \mathbf{O}_{m_{\mathrm{P}} \times m_{\mathrm{S}}} & \mathbf{\Omega}_{\mathrm{P}}^2 + \mathbf{k}_{\mathrm{PP}} \end{array}\right] ; \tag{8b}$$

$$\mathbf{g} = -\mathbf{\Gamma}^{\top} \cdot \mathbf{M} \cdot \boldsymbol{\tau} = -\left[\begin{array}{c} \mathbf{p}_{\mathrm{S}} \\ \hdashline \mathbf{p}_{\mathrm{P}} + \mathbf{p}_{\mathrm{PP}} \end{array}\right] , \tag{8c}$$

in which $\mathbf{p}_{\mathrm{S}} = \mathbf{\Phi}_{\mathrm{S}}^{\top} \cdot \mathbf{M}_{\mathrm{S}} \cdot \boldsymbol{\tau}_{\mathrm{S}}$ and $\mathbf{p}_{\mathrm{P}} = \mathbf{\Phi}_{\mathrm{P}}^{\top} \cdot \mathbf{M}_{\mathrm{P}} \cdot \boldsymbol{\tau}_{\mathrm{P}}$ are the two arrays collecting the modal participation factors for S and P, respectively. The presence of the S subsystem affects the mass, stiffness and participation factors of the P structure, through the additional blocks:

$$\mathbf{m}_{\mathrm{PP}} = \mathbf{\Psi}_{\mathrm{SP}}^{\top} \cdot \mathbf{M}_{\mathrm{S}} \cdot \mathbf{\Psi}_{\mathrm{SP}} \,; \tag{9a}$$

$$\mathbf{k}_{\mathrm{PP}} = \mathbf{\Phi}_{\mathrm{P}}^{\top} \cdot \left[\mathbf{K}_{\mathrm{PP}} \cdot \mathbf{\Phi}_{\mathrm{P}} + \mathbf{K}_{\mathrm{SP}}^{\top} \cdot \mathbf{\Psi}_{\mathrm{SP}}\right] \,; \tag{9b}$$

$$\mathbf{p}_{\mathrm{PP}} = \mathbf{\Psi}_{\mathrm{SP}}^{\top} \cdot \mathbf{M}_{\mathrm{S}} \cdot \boldsymbol{\tau}_{\mathrm{S}} \,. \tag{9c}$$

Furthermore, the P-S coupling is established in the reduced modal space by the out-of-diagonal block $\mathbf{m}_{\mathrm{SP}}$, given by:

$$\mathbf{m}_{\mathrm{SP}} = \mathbf{\Phi}_{\mathrm{S}}^{\top} \cdot \mathbf{M}_{\mathrm{S}} \cdot \mathbf{\Psi}_{\mathrm{SP}} \,. \tag{10}$$

Notably:

- Modal frequencies and modal shapes of the coupled (undamped) P-S dynamic system are the solution of the real-valued eigenproblem:

$$\mathbf{m} \cdot \mathbf{\Phi} \cdot \mathbf{\Omega}^2 = \mathbf{k} \cdot \mathbf{\Phi} \,. \tag{11}$$

- The blocks of Eqs. (9) and (10) account for the dynamic feedback between the two components, and neglecting their contribution leads to the cascaded approximation.

## 2.2 Criteria on the number of vibrational modes

In practical applications, a limited number of modes are retained in the dynamic analysis, typically the ones significantly contributing to the seismic motion. This leads to the MDM, in which the truncated modes result in an approximated structural response and may introduce considerable inaccuracies in the high-frequency range. Current codes of practice (e.g. Eurocode [9]) set out truncation thresholds via a set of criteria in which: (i) all modes with effective modal masses greater than 5% of the total mass need to be considered; and (ii) the sum of the effective modal masses for the retained modes, amounts to at least 90% of the total mass of the structure. These conditions can be expressed on the two subsystems in turn as:

$$\max\left\{\mathbf{p}_{\mathrm{t_P}}\right\} < \sqrt{0.05 M_{\mathrm{P}}}\,; \quad \max\left\{\mathbf{p}_{\mathrm{t_S}}\right\} < \sqrt{0.05 M_{\mathrm{S}}}\,, \tag{12}$$

where $\mathbf{p}_{\mathrm{t_P}}$ and $\mathbf{p}_{\mathrm{t_S}}$ comprise the arrays listing the modal participation factors for the truncated modes of P and S, respectively. Similarly:

$$\sum_{i=1}^{m_{\mathrm{P}}} \left\{\mathbf{p}_{\mathrm{P}}\right\}_i^2 \geqslant 0.9 M_{\mathrm{P}}\,; \quad \sum_{j=1}^{m_{\mathrm{S}}} \left\{\mathbf{p}_{\mathrm{S}}\right\}_j^2 \geqslant 0.9 M_{\mathrm{S}}\,. \tag{13}$$

## 2.3 Modal correction method

It has been noted [16] that such criteria may fail in terms of stresses and strains, leading to significant errors in the design values of various checks. Moreover, these criteria cannot easily be adopted for secondary systems, which may possess numerous low-frequency modes with negligible mass. Accordingly, it is possible to improve the accuracy via a correction term appended to the approximate response (Eq. (3)) such that:

$$\mathbf{u}(t) = \widetilde{\mathbf{u}}(t) + \Delta\mathbf{u}\,(t)\ . \tag{14a}$$

Two alternative formulations can be adopted for the modal correction term $(\Delta\mathbf{u})$ to account for the contribution of the neglected modes:

$$\Delta\mathbf{u}_{\mathrm{MAM}}\,(t) = \Delta\mathbf{b}\,\ddot{u}_g\,(t)\ ; \quad \Delta\mathbf{u}_{\mathrm{DyMAM}}\,(t) = \Delta\mathbf{b}\,\omega_{\mathrm{F}}^2\,\theta\,(t)\ , \tag{14b}$$

corresponding to the MAM and DyMAM, respectively, where $\Delta\mathbf{b}$ is the static correction vector:

$$\Delta\mathbf{b} = \mathbf{b}_{\mathrm{G}} - \boldsymbol{\Gamma}\cdot\mathbf{b}_{\mathrm{M}}\,, \tag{14c}$$

in which $\mathbf{b}_{\mathrm{G}} = -\mathbf{K}^{-1}\cdot\mathbf{M}\cdot\boldsymbol{\tau} = \left\{ \{\mathbf{b}_{\mathrm{S}} + \mathbf{N}_{\mathrm{SP}}\cdot\mathbf{b}_{\mathrm{P}}\}^{\top} \vdots \mathbf{b}_{\mathrm{P}}^{\top} \right\}^{\top}$ and $\mathbf{b}_{\mathrm{M}} = \mathbf{k}^{-1}\cdot\mathbf{g}$ are the static response of the whole structure, and the response due to the modes of vibration retained in analysis (neglecting the inertial effects in Eqs. (1) and (7)), respectively, while $\mathbf{b}_{\mathrm{S}}$ and $\mathbf{b}_{\mathrm{P}}$ are solutions of:

$$\mathbf{K}_{\mathrm{S}}\cdot\mathbf{b}_{\mathrm{S}} = -\mathbf{M}_{\mathrm{S}}\cdot\boldsymbol{\tau}_{\mathrm{S}}\,; \quad \left[\mathbf{K}_{\mathrm{P}} + \mathbf{K}_{\mathrm{PP}} + \mathbf{K}_{\mathrm{SP}}^{\top}\cdot\mathbf{N}_{\mathrm{SP}}\right]\mathbf{b}_{\mathrm{P}} = -\mathbf{M}_{\mathrm{P}}\cdot\boldsymbol{\tau}_{\mathrm{P}} - \mathbf{K}_{\mathrm{SP}}^{\top}\cdot\mathbf{b}_{\mathrm{S}}\,, \tag{14d}$$

and $\theta(t)$ is the response of a single-degree-of-freedom (SDoF) oscillator satisfying:

$$\ddot{\theta}\,(t) + 2\,\zeta_{\mathrm{F}}\,\omega_{\mathrm{F}}\,\dot{\theta}\,(t) + \omega_{\mathrm{F}}^{2}\,\theta\,(t) = \ddot{u}_{g}\,(t)\ , \tag{15a}$$

in which $\omega_{\mathrm{F}}$ and $\zeta_{\mathrm{F}}$ are chosen as:

$$\omega_{\mathrm{F}} = 2\min\left\{\boldsymbol{\Omega}_{\mathrm{P}}\right\}\ ; \quad \zeta_{\mathrm{F}} = \frac{1}{\sqrt{2}}\,. \tag{15b}$$

## 2.4 Construction of viscous damping matrix

Assuming viscously damped linear systems, it is possible to assemble the equivalent viscous damping matrix as:

$$\mathbf{C} = \left[\begin{array}{c:c} \mathbf{C}_{\mathrm{S}} & \mathbf{C}_{\mathrm{SP}} \\ \hdashline \mathbf{C}_{\mathrm{SP}}^{\top} & \mathbf{C}_{\mathrm{P}} + \mathbf{C}_{\mathrm{PP}} \end{array}\right]\ ; \quad \mathbf{c} = \boldsymbol{\Gamma}^{\top}\cdot\mathbf{C}\cdot\boldsymbol{\Gamma} = \left[\begin{array}{c:c} \mathbf{c}_{\mathrm{S}} & \mathbf{c}_{\mathrm{SP}} \\ \hdashline \mathbf{c}_{\mathrm{SP}}^{\top} & \mathbf{c}_{\mathrm{P}} + \mathbf{c}_{\mathrm{PP}} \end{array}\right]\,, \tag{16}$$

where $\{\mathbf{C}_{\mathrm{S}}, \mathbf{C}_{\mathrm{P}}\}$ and $\{\mathbf{c}_{\mathrm{S}}, \mathbf{c}_{\mathrm{P}}\}$ represent the corresponding damping matrices on S and P in the geometrical and modal domain, respectively; $\mathbf{C}_{\mathrm{SP}}$ is the damping matrix coupling the two subsystems; $\mathbf{C}_{\mathrm{PP}}$ represents the residual damping in the P substructure due to the presence of the S subsystem. Three alternative formulations can be adopted for constructing the individual blocks, and these are described in the following subsections. Once the associated matrices are defined, the combined response of the P-S system will then be governed by:

$$\mathbf{m}\cdot\ddot{\mathbf{q}}(t) + \mathbf{c}\cdot\dot{\mathbf{q}}(t) + \mathbf{k}\cdot\mathbf{q}(t) = \mathbf{g}\,\ddot{u}_{g}(t)\,. \tag{17}$$

### 2.4.1 Rayleigh damping

The Rayleigh damping model is adopted for the two subsystems so the matrices $\mathbf{C}_{\mathrm{S}}$ and $\mathbf{C}_{\mathrm{P}}$ take the form:

$$\mathbf{C}_{\mathrm{S}} = \zeta_{\mathrm{S}}\,\left[\alpha_{\mathrm{M}}\,\mathbf{M}_{\mathbf{S}} + \alpha_{\mathrm{K}}\,\mathbf{K}_{\mathbf{S}}\right]\ ; \quad \mathbf{C}_{\mathrm{P}} = \zeta_{\mathrm{P}}\,\left[\alpha_{\mathrm{M}}\,\mathbf{M}_{\mathbf{P}} + \alpha_{\mathrm{K}}\,\mathbf{K}_{\mathbf{P}}\right]\,, \tag{18a}$$

in which $\zeta_{\rm S}$ and $\zeta_{\rm P}$ are the viscous damping ratios for S and P, respectively, while $\alpha_{\rm M}$ and $\alpha_{\rm K}$ are the coefficients of proportionality for mass and stiffness, evaluated as:

$$\alpha_{\rm M} = \frac{2\,\omega_{\rm I}\,\omega_{\rm II}}{\omega_{\rm I}+\omega_{\rm II}}\,b\,; \quad \alpha_{\rm K} = \frac{2}{\omega_{\rm I}+\omega_{\rm II}}\,b\,; \quad b = \frac{2\,(\omega_{\rm II}^2-\omega_{\rm I}^2)}{\omega_{\rm II}^2-\omega_{\rm I}^2+2\,\omega_{\rm I}\,\omega_{\rm II}\ln\left(\omega_{\rm II}/\omega_{\rm I}\right)}\,, \tag{18b}$$

where $\omega_{\rm I}$ and $\omega_{\rm II}$ are chosen circular frequencies of $\omega_{\rm I,S}$, $\omega_{\rm I,P}$ and $\omega_{\rm II,S}$, $\omega_{\rm II,P}$ for S and P, respectively, such that average values of $\zeta_{\rm S}$ and $\zeta_{\rm P}$ are achieved in the corresponding intervals $[\omega_{\rm I,S},\omega_{\rm II,S}]$, $[\omega_{\rm I,P},\omega_{\rm II,P}]$. A single interval, $[\min\{\omega_{\rm I,S},\omega_{\rm I,P}\},\min\{\omega_{\rm II,S},\omega_{\rm II,S}\}]$ can alternatively be assumed for the circular frequencies of both components. Additionally, the coupling matrix takes the form of $\mathbf{C}_{\rm SP}=\zeta_{\rm S}\,\alpha_{\rm K,S}\,\mathbf{K}_{\rm SP}$, while the residual damping in the P substructure is $\mathbf{C}_{\rm PP}=\zeta_{\rm S}\,\alpha_{\rm K,S}\,\mathbf{K}_{\rm PP}$.

In the modal subdomain $\mathbf{c}_{\rm S}$ and $\mathbf{c}_{\rm P}$ are given (similar to Eqs. (18a)) by:

$$\mathbf{c}_{\rm S} = \zeta_{\rm S}\,\left[\alpha_{\rm M,S}\,\mathbf{I}_{\rm m_S}+\alpha_{\rm K,S}\,\mathbf{\Omega}_{\rm S}^2\right]\,; \quad \mathbf{c}_{\rm P} = \zeta_{\rm P}\,\left[\alpha_{\rm M,P}\,\mathbf{I}_{\rm m_P}+\alpha_{\rm K,P}\,\mathbf{\Omega}_{\rm P}^2\right]\,. \tag{19a}$$

Furthermore, the presence of the S subsystem affects the damping of the P structure, through the additional block:

$$\mathbf{c}_{\rm PP} = \zeta_{\rm S}\,\left[\alpha_{\rm M,S}\,\mathbf{m}_{\rm PP}+\alpha_{\rm K,S}\,\mathbf{k}_{\rm PP}\right]\,, \tag{19b}$$

while, the P-S coupling is established by the out-of-diagonal block $\mathbf{c}_{\rm SP}$, given by:

$$\mathbf{c}_{\rm SP} = \zeta_{\rm S}\,\alpha_{\rm M,S}\,\mathbf{m}_{\rm SP}\,. \tag{19c}$$

### 2.4.2 Caughey damping

It is possible to define damping ratios for a higher number of modes. Retaining the first four terms of the Caughey series, one can deduce:

$$\mathbf{C}_{\rm S} = \alpha_{\rm S,0}\,\mathbf{M}_{\rm S}+\alpha_{\rm S,1}\,\mathbf{K}_{\rm S}+\mathbf{M}_{\rm S}\sum_{l=2}^{3}a_{{\rm S},l}\,\left[\mathbf{\Phi}_{\rm S}\cdot\mathbf{\Phi}_{\rm S}^{\top}\cdot\mathbf{K}_{\rm S}\right]^{l}\,, \tag{20a}$$

$$\mathbf{C}_{\rm P} = \alpha_{\rm P,0}\,\mathbf{M}_{\rm P}+\alpha_{\rm P,1}\,\mathbf{K}_{\rm P}+\mathbf{M}_{\rm P}\sum_{l=2}^{3}a_{{\rm P},l}\,\left[\mathbf{\Phi}_{\rm P}\cdot\mathbf{\Phi}_{\rm P}^{\top}\cdot\mathbf{K}_{\rm P}\right]^{l}\,, \tag{20b}$$

for the S and P subsystems, respectively, while the coupling and residual matrices take the form:

$$\mathbf{C}_{\rm SP} = \alpha_{\rm S,1}\,\mathbf{K}_{\rm SP}\,; \quad \mathbf{C}_{\rm PP} = \alpha_{\rm S,1}\,\mathbf{K}_{\rm PP}\,, \tag{20c}$$

where the coefficients $\alpha_{\rm S}$ and $\alpha_{\rm P}$ satisfy the succeeding algebraic equations:

$$\zeta_{{\rm S},\,i} = \frac{1}{2}\sum_{l=0}^{3} a_{{\rm S},l}\,\omega_{{\rm S},i}^{2l-1}\,; \quad \zeta_{{\rm P},\,i} = \frac{1}{2}\sum_{l=0}^{3} a_{{\rm P},l}\,\omega_{{\rm P},i}^{2l-1}\,; \quad i = \{i_1,\ldots,i_4\}\,, \tag{20d}$$

with $\zeta_{{\rm S},i}$, $\zeta_{{\rm P},i}$ being the $i^{\rm th}$ modal damping ratios corresponding to chosen frequencies $\omega_{\rm S,i}$, $\omega_{\rm P,i}$, for S and P systems, respectively. Once projected on to the modal subdomain, the corresponding blocks read:

$$\mathbf{c}_{\rm S} = \alpha_{{\rm S},0}\,\mathbf{I}_{m_{\rm S}} + \alpha_{{\rm S},1}\,\boldsymbol{\Omega}_{\rm S}^2 + \boldsymbol{\Phi}_{\rm S}^{\top}\cdot\mathbf{R}_{\rm S}\cdot\boldsymbol{\Phi}_{\rm S}\,; \quad \mathbf{c}_{\rm P} = \alpha_{{\rm P},0}\,\mathbf{I}_{m_{\rm P}} + \alpha_{{\rm P},1}\,\boldsymbol{\Omega}_{\rm P}^2 + \boldsymbol{\Phi}_{\rm P}^{\top}\cdot\mathbf{R}_{\rm P}\cdot\boldsymbol{\Phi}_{\rm P}\,; \tag{21a}$$

$$\mathbf{c}_{\rm SP} = \alpha_{{\rm S},0}\,\mathbf{m}_{\rm SP} + \boldsymbol{\Phi}_{\rm S}^{\top}\cdot\mathbf{R}_{\rm S}\cdot\boldsymbol{\Psi}_{\rm SP}\,; \quad \mathbf{c}_{\rm PP} = \alpha_{{\rm S},0}\,\mathbf{m}_{\rm PP} + \alpha_{{\rm S},1}\,\mathbf{k}_{\rm PP} + \boldsymbol{\Psi}_{\rm SP}^{\top}\cdot\mathbf{R}_{\rm S}\cdot\boldsymbol{\Psi}_{\rm SP}\,; \tag{21b}$$

$$\mathbf{R}_{\rm S} = \mathbf{M}_{\rm S}\sum_{l=2}^{3}\alpha_{{\rm S},l}\left[\boldsymbol{\Phi}_{\rm S}\cdot\boldsymbol{\Phi}_{\rm S}^{\top}\cdot\mathbf{K}_{\rm S}\right]^{l}\,; \quad \mathbf{R}_{\rm P} = \mathbf{M}_{\rm P}\sum_{l=2}^{3}\alpha_{{\rm P},l}\left[\boldsymbol{\Phi}_{\rm P}\cdot\boldsymbol{\Phi}_{\rm P}^{\top}\cdot\mathbf{K}_{\rm P}\right]^{l}\,. \tag{21c}$$

Evidently, when the first two terms are only considered the damping model reduces to the case of Rayleigh. Additionally, the selection of four modes is driven by the requirement to maintain positive $\zeta$ outside the chosen interval, while at the same time avoid ill-conditioning associated with higher mode number [15].

### 2.4.3 Constant modal damping

An alternative formulation can be adopted for constructing the viscous damping matrix. Considering constant damping on the vibrational modes retained, $\mathbf{c}_{\rm S}$ and $\mathbf{c}_{\rm P}$ can be expressed as:

$$\mathbf{c}_{\rm S} = 2\,\zeta_{\rm S}\,\boldsymbol{\Omega}_{\rm S}\,; \quad \mathbf{c}_{\rm P} = 2\,\zeta_{\rm P}\,\boldsymbol{\Omega}_{\rm P}\,, \tag{22a}$$

while the coupling and residual matrices can be expressed as:

$$\mathbf{c}_{\rm SP} = \mathbf{O}_{m_{\rm S}\times m_{\rm P}}\,; \quad \mathbf{c}_{\rm PP} = 2\,\kappa_{\rm S}\,\mathbf{k}_{\rm PP}\,. \tag{22b}$$

The corresponding blocks associated with the individual subsystems can then be assembled in the geometric space as:

$$\mathbf{C}_{\rm S} = \widetilde{\mathbf{C}}_{\rm S} + \Delta\mathbf{C}_{\rm S}\,; \quad \mathbf{C}_{\rm P} = \widetilde{\mathbf{C}}_{\rm P} + \Delta\mathbf{C}_{\rm P}\,, \tag{23a}$$

and similarly:

$$\mathbf{C}_{\mathrm{SP}} = \widetilde{\mathbf{C}}_{\mathrm{SP}} + \Delta\mathbf{C}_{\mathrm{SP}}\,; \quad \mathbf{C}_{\mathrm{PP}} = \widetilde{\mathbf{C}}_{\mathrm{PP}} + \Delta\mathbf{C}_{\mathrm{PP}}\,, \tag{23b}$$

where blocks with the overtilde are those associated with the modes retained in the modal analysis ($m_{\mathrm{S}}$ for the S subsystem and $m_{\mathrm{P}}$ for the P substructure), and the ones denoted by $\Delta$ account for the higher modes. Based on the preceding expressions, one can derive:

$$\widetilde{\mathbf{C}}_{\mathrm{S}} = 2\,\zeta_{\mathrm{S}}\,\mathbf{M}_{\mathrm{S}}\cdot\boldsymbol{\Phi}_{\mathrm{S}}\cdot\boldsymbol{\Omega}_{\mathrm{S}}\cdot\boldsymbol{\Phi}_{\mathrm{S}}^{\top}\cdot\mathbf{M}_{\mathrm{S}}\,; \quad \widetilde{\mathbf{C}}_{\mathrm{P}} = 2\,\zeta_{\mathrm{P}}\,\mathbf{M}_{\mathrm{P}}\cdot\boldsymbol{\Phi}_{\mathrm{P}}\cdot\boldsymbol{\Omega}_{\mathrm{P}}\cdot\boldsymbol{\Phi}_{\mathrm{P}}^{\top}\cdot\mathbf{M}_{\mathrm{P}}\,; \tag{24a}$$

$$\widetilde{\mathbf{C}}_{\mathrm{SP}} = -\widetilde{\mathbf{C}}_{\mathrm{S}}\cdot\boldsymbol{\Psi}_{\mathrm{SP}}\cdot\boldsymbol{\Phi}_{\mathrm{P}}^{\top}\cdot\mathbf{M}_{\mathrm{P}}\,; \tag{24b}$$

$$\widetilde{\mathbf{C}}_{\mathrm{PP}} = \mathbf{M}_{\mathrm{P}}\cdot\boldsymbol{\Phi}_{\mathrm{P}}\left[\boldsymbol{\Psi}_{\mathrm{SP}}^{\top}\cdot\widetilde{\mathbf{C}}_{\mathrm{S}}\cdot\boldsymbol{\Psi}_{\mathrm{SP}} + 2\,\kappa_{\mathrm{S}}\,\mathbf{k}_{\mathrm{PP}}\right]\boldsymbol{\Phi}_{\mathrm{P}}^{\top}\cdot\mathbf{M}_{\mathrm{P}}\,. \tag{24c}$$

Additionally, it is possible to derive the expressions for the higher mode contribution by adopting the Rayleigh damping model as:

$$\Delta\mathbf{C}_{\mathrm{S}} = \mu_{\mathrm{S}}\,\Delta\mathbf{M}_{\mathrm{S}} + \kappa_{\mathrm{S}}\,\Delta\mathbf{K}_{\mathrm{S}}\,; \quad \Delta\mathbf{C}_{\mathrm{P}} = \mu_{\mathrm{P}}\,\Delta\mathbf{M}_{\mathrm{P}} + \kappa_{\mathrm{P}}\,\Delta\mathbf{K}_{\mathrm{P}}\,; \tag{25a}$$

$$\Delta\mathbf{C}_{\mathrm{SP}} = \kappa_{\mathrm{S}}\,\Delta\mathbf{K}_{\mathrm{SP}}\,; \quad \Delta\mathbf{C}_{\mathrm{PP}} = \kappa_{\mathrm{S}}\,\Delta\mathbf{K}_{\mathrm{PP}} - \mu_{\mathrm{S}}\,\widetilde{\mathbf{M}}_{\mathrm{PP}}\,, \tag{25b}$$

where $\{\mu_{\mathrm{S}}, \kappa_{\mathrm{S}}\}$ and $\{\mu_{\mathrm{P}}, \kappa_{\mathrm{P}}\}$ are the pairs of coefficients for the damping model applied to the S and P components, in turn, such that:

$$\mu_{\mathrm{S}} = \zeta_{\mathrm{S}}\,\omega_{\mathrm{S,max}}\,; \quad \kappa_{\mathrm{S}} = \zeta_{\mathrm{S}}/\omega_{\mathrm{S,max}}\,; \quad \omega_{\mathrm{S,max}} = \max\left[\boldsymbol{\Omega}_{\mathrm{S}}\right] = \omega_{\mathrm{S},m_{\mathrm{S}}}\,; \tag{26a}$$

$$\mu_{\mathrm{P}} = \zeta_{\mathrm{P}}\,\omega_{\mathrm{P,max}}\,; \quad \kappa_{\mathrm{P}} = \zeta_{\mathrm{P}}/\omega_{\mathrm{P,max}}\,; \quad \omega_{\mathrm{P,max}} = \max\left[\boldsymbol{\Omega}_{\mathrm{P}}\right] = \omega_{\mathrm{P},m_{\mathrm{P}}}\,, \tag{26b}$$

while the residual modal contributions can be posed in the form:

$$\Delta\mathbf{M}_{\mathrm{S}} = \mathbf{M}_{\mathrm{S}} - \widetilde{\mathbf{M}}_{\mathrm{S}}\,; \quad \Delta\mathbf{M}_{\mathrm{P}} = \mathbf{M}_{\mathrm{P}} - \widetilde{\mathbf{M}}_{\mathrm{P}}\,; \tag{27a}$$

$$\Delta\mathbf{K}_{\mathrm{S}} = \mathbf{K}_{\mathrm{S}} - \widetilde{\mathbf{K}}_{\mathrm{S}}\,; \quad \boldsymbol{\Delta}\mathbf{K}_{\mathrm{P}} = \mathbf{K}_{\mathrm{P}} - \widetilde{\mathbf{K}}_{\mathrm{P}}\,; \tag{27b}$$

$$\Delta\mathbf{K}_{\mathrm{SP}} = \mathbf{K}_{\mathrm{SP}} - \widetilde{\mathbf{K}}_{\mathrm{SP}}\,; \quad \Delta\mathbf{K}_{\mathrm{PP}} = \mathbf{K}_{\mathrm{PP}} - \widetilde{\mathbf{K}}_{\mathrm{PP}}\,, \tag{27c}$$

in which the blocks with the overtilde are evaluated as:

$$\widetilde{\mathbf{M}}_{\mathrm{S}} = \mathbf{M}_{\mathrm{S}} \cdot \boldsymbol{\Phi}_{\mathrm{S}} \cdot \boldsymbol{\Phi}_{\mathrm{S}}^{\top} \cdot \mathbf{M}_{\mathrm{S}} \,; \quad \widetilde{\mathbf{M}}_{\mathrm{P}} = \mathbf{M}_{\mathrm{P}} \cdot \boldsymbol{\Phi}_{\mathrm{P}} \cdot \boldsymbol{\Phi}_{\mathrm{P}}^{\top} \cdot \mathbf{M}_{\mathrm{P}} \,; \tag{28a}$$

$$\widetilde{\mathbf{K}}_{\mathrm{S}} = \mathbf{M}_{\mathrm{S}} \cdot \boldsymbol{\Phi}_{\mathrm{S}} \cdot \boldsymbol{\Omega}_{\mathrm{S}}^{2} \cdot \boldsymbol{\Phi}_{\mathrm{S}}^{\top} \cdot \mathbf{M}_{\mathrm{S}} \,; \quad \widetilde{\mathbf{K}}_{\mathrm{P}} = \mathbf{M}_{\mathrm{P}} \cdot \boldsymbol{\Phi}_{\mathrm{P}} \cdot \boldsymbol{\Omega}_{\mathrm{P}}^{2} \cdot \boldsymbol{\Phi}_{\mathrm{P}}^{\top} \cdot \mathbf{M}_{\mathrm{P}} \,; \tag{28b}$$

$$\widetilde{\mathbf{K}}_{\mathrm{SP}} = -\widetilde{\mathbf{K}}_{\mathrm{S}} \cdot \boldsymbol{\Psi}_{\mathrm{SP}} \cdot \boldsymbol{\Phi}_{\mathrm{P}}^{\top} \cdot \mathbf{M}_{\mathrm{P}} \,; \tag{28c}$$

$$\widetilde{\mathbf{K}}_{\mathrm{PP}} = \mathbf{M}_{\mathrm{P}} \cdot \boldsymbol{\Phi}_{\mathrm{P}} \left[ \boldsymbol{\Psi}_{\mathrm{SP}}^{\top} \cdot \widetilde{\mathbf{K}}_{\mathrm{S}} \cdot \boldsymbol{\Psi}_{\mathrm{SP}} + \mathbf{k}_{\mathrm{PP}} \right] \boldsymbol{\Phi}_{\mathrm{P}}^{\top} \cdot \mathbf{M}_{\mathrm{P}} \,; \tag{28d}$$

$$\widetilde{\mathbf{M}}_{\mathrm{PP}} = \mathbf{M}_{\mathrm{P}} \cdot \boldsymbol{\Phi}_{\mathrm{P}} \cdot \boldsymbol{\Psi}_{\mathrm{SP}}^{\top} \left[ \mathbf{M}_{\mathrm{S}} - \widetilde{\mathbf{M}}_{\mathrm{S}} \right] \boldsymbol{\Psi}_{\mathrm{SP}} \cdot \boldsymbol{\Phi}_{\mathrm{P}}^{\top} \cdot \mathbf{M}_{\mathrm{P}} \,. \tag{28e}$$

Notably, Eqs. (25) to (28), constitute a novel characterisation of the truncated vibrational mode contribution, that is deemed necessary in formulating a consistent viscous damping matrix for the primary-secondary assembly.

# 3 Application

Aimed at assessing the validity of the formulation presented in the previous section, the seismic response of coupled P-S systems has numerically been investigated via a representative case study, and the results are reported and discussed in this section.

## 3.1 Modelling

Figure 1 shows the composite system under investigation, which consists of a two-dimensional 5-storey moment-resisting frame (P) multiply connected with flexible links to a MDoF staircase system (S). Self-weight and super-dead load are the two sources of mass, concentrated at the floor level for the P structure and uniformly distributed for the S subsystem, while mass at the P-S interface is assumed to act on the P structure. The total masses are $M_P = 99.8\,\mathrm{Mg}$ and $M_S = 47.0\,\mathrm{Mg}$ and the resulting S-P mass ratio is $\mu = M_{\mathrm{S}}/M_{\mathrm{P}} = 0.47$. The fundamental periods of vibration are $T_{P,1} = 0.215\,\mathrm{s}$ for the P structure and $T_{S,1} = 0.312\,\mathrm{s}$ for the S sub-model (the latter being fixed to the ground as well as to the points of connection to P).

The total number of DoFs is $n = n_p + n_s = 30 + 78 = 108$, and $m = m_p + m_s = 4 + 6 = 10$ modes (9%) were retained in the analysis, so that 98% and 87% of the modal mass for each sub-model, respectively, participates in the seismic motion in the direction of interest ($x$ for our analyses). In order to trigger the P-S dynamic interaction for an accelerogram applied along $x$, the 5th mode of the S subsystem, with a large participation mass in the direction of interest, has been tuned to the fundamental

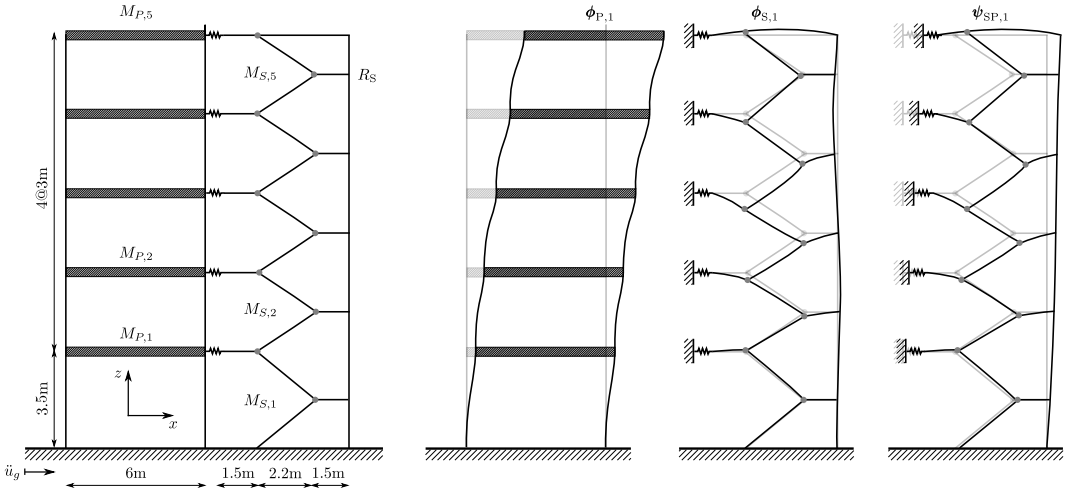


Figure 1: Primary-secondary case-study model.

Table 1: Ground motion records

| Earthquake | Site / Component | $\Delta t$ [s] | PGA [$g$] |
|---|---|---|---|
| Imperial Valley 1940 | El Centro / 180 | 0.0100 | 0.258 |
| Erzican 1992 | Erzican / N-S | 0.0050 | 0.489 |
| Irpinia 1980 | Calitri / 270 | 0.0024 | 0.152 |

mode of the P frame, which accounts for about $84\%$ of $M_{\mathrm{P}}$ in the $x$ direction, so that $T_{P,1} = T_{S,5}$.

## 3.2 Damping characterisation

Four variants of the viscous damping matrix are studied, namely: Rayleigh; defined via (i) single and (ii) paired intervals for P and S; (iii) Caughey; and (iv) Modal. To enable a fair assessment of the MSM method to each variant, exact-reference damping models are defined, in which all modes are retained for the case of modal damping (i.e. $m_S = n_S$, $m_P = n_P$); the circular frequencies of the associated Rayleigh intervals are taken as $\omega_{\mathrm{I,S}} = \omega_{\mathrm{S},4}$, $\omega_{\mathrm{II,S}} = \omega_{\mathrm{S},10}$ and $\omega_{\mathrm{I,P}} = \omega_{\mathrm{P},1}$, $\omega_{\mathrm{II,P}} = \omega_{\mathrm{P},2}$ for S and P, respectively; the modes for Caughey are $i_{\mathrm{S}} = \{4, 5, 6, 8\}$ and $i_{\mathrm{P}} = \{1, 2, 3, 4\}$. Once the MDM is considered, $\omega_{\mathrm{II},S} = \omega_{\mathrm{S},6}$ and $i_{\mathrm{S}} = \{3, 4, 5, 6\}$. The reference values of the viscous damping ratios are $\zeta_{\mathrm{P}} = \zeta_{\mathrm{S}} = 0.05$, thus allowing the construction of the damping models for the full dynamic P-S system in accordance with the proposed formulation.

## 3.3 Numerical analyses

A series of linear dynamic analyses were carried out using the commercial software SAP2000 [19] to build the relevant mass and stiffness matrices and the numerical software MATLAB [20] to implement the MSM variant described in the previous section. Three recorded accelerograms were used, namely El Centro 1940, Erzican 1992 and Irpinia 1980 (details are listed in Table 1). These records have been chosen because of their distinct characteristics, which allow exploring the performance of the combined P-S system under different loading scenarios and can be used to identify general trends in the results.

The validity of the MSM has initially been confirmed in the frequency domain, with the exact responses of the various damping models applied on individual systems (modal damping also applied on the full dynamic P-S system), being compared to that of a hysteretic model [21] (whose evaluation is only permitted in the frequency domain), treated here as a reference one, as is believed to be in better accordance with experimental data. The corresponding truncated (MDM) responses were then evaluated for each damping model and were compared with the analogous corrected ones (MAM, DyMAM) (§ 3.4). Finally, the effects on the dynamic response were quantified in the time domain (§ 3.5). In accordance with performance-based earthquake engineering principles [22], different S components can be sensitive to different engineering demand parameters (EDPs) which can often be used to assess the expected performance. In the present study, they have been selected as: the maximum relative displacements, $u_{\mathrm{S}}$; and the maximum absolute accelerations, $\ddot{u}_{\mathrm{S}}$ in the S sub-model. Point $R_{\mathrm{S}}$ in Figure 1 identifies the position where the EDPs have been calculated.

## 3.4 Frequency-domain response

A selection of results is presented in this section for the case study under consideration. The frequency response function (FRF) has been evaluated for a representative DoF in the secondary system, i.e. the $x$ displacement of point $R_{\mathrm{S}}$ (see Fig. 1). Fig. 2(a) shows the exact FRF in the geometric space, for the various damping models studied, whose cumulative relative differences are then reported (Fig. 2(b)) with respect to the hysteretic model. It is evident that there are variations in the magnitude of the fundamental frequency ($\omega \approx 22$ rad/s) which is overestimated by the modal, Rayleigh and Caughey models applied on individual subsystems, while the paired Rayleigh and full combined system appear to be in better agreement with the hysteretic.

Figure 3 compares the FRF as evaluated for each of the models, for five levels of approximation, namely: the full MSM, which can be regarded as the exact solution; the cascaded approximation (light dashed line), where the P-S dynamic interaction is neglected; the MDM where no correction is applied (light solid line); the MAM (dotted line) and the proposed DyMAM (dark dotted line), introducing a static and dynamic correction, respectively. It is observed that the response predicted by the cascaded approximation always introduces a significant inaccuracy in the low-frequency range, leading to an overestimation of the fundamental frequency. This is due to the

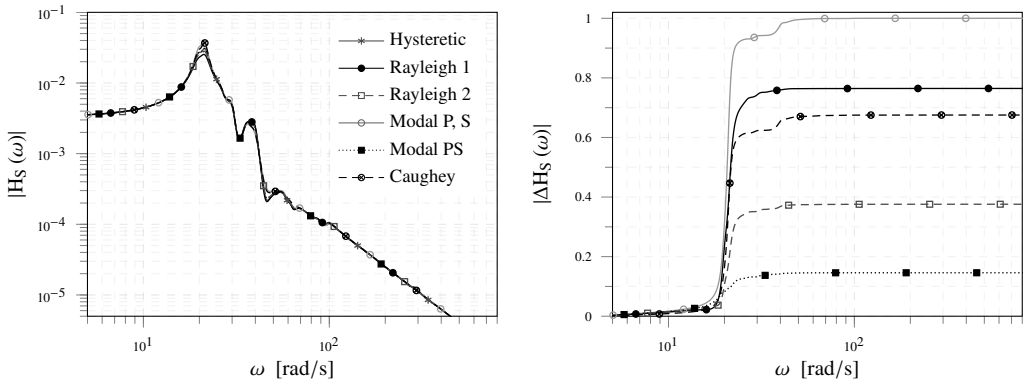


(a) (b)

Figure 2: Exact FRF for various damping models (a), and corresponding cumulative differences (b) quantified on S.

high S-P mass ratio ($\mu = 0.47$), suggesting that the dynamic interaction must indeed be accounted for. Consequently, the cascaded approximation is not considered in any of the subsequent stages of the analyses.

Figure 4 quantifies the cumulative inaccuracies of the remaining three approximations, normalised with the maximum one, for each model. As expected, the truncation is shown to induce an error, as predicted by the MDM for all models. Notably, while MAM is shown to improve the dynamic response in the low-frequency range, a large discrepancy is introduced in the high-frequency range (clearly seen in Fig. 3, at $\omega \approx 145$ rad/s). Interestingly, the proposed DyMAM is capable of sustaining the correction in the low-frequency range and concurrently ameliorating the error in the high-frequency domain. A discrepancy of the DyMAM shown at $\omega > 170$ rad/s in Fig. 3(a) can indeed be regarded as negligible (see Fig. 3(b)).

## 3.5 Time-domain response

The dynamic analysis was carried out in the time domain, for the system under investigation and the three input accelerograms. The displacement and acceleration response histories have been computed for the MDM, MAM and DyMAM approximations. Figure 5 compares the corresponding discrepancies for the case of modal damping evolving with time, while Fig. 6 reports the cumulative values normalised with the associated maxima, at the end of the time interval. One can observe that when displacements are under consideration, the highest accumulated error is given by the MDM, while conversely larger discrepancies are predicted for the case of acceleration EDPs. Interestingly, the DyMAM consistently diminishes errors, a result that appears of practical importance as it highlights its appropriateness to the various engineering demand parameters chosen for the analysis of a given subsystem. It is also worth emphasising that, notwithstanding its implementation in this paper, the application of the MAM to the case of accelerations is currently hindered to the practitioner, due to its

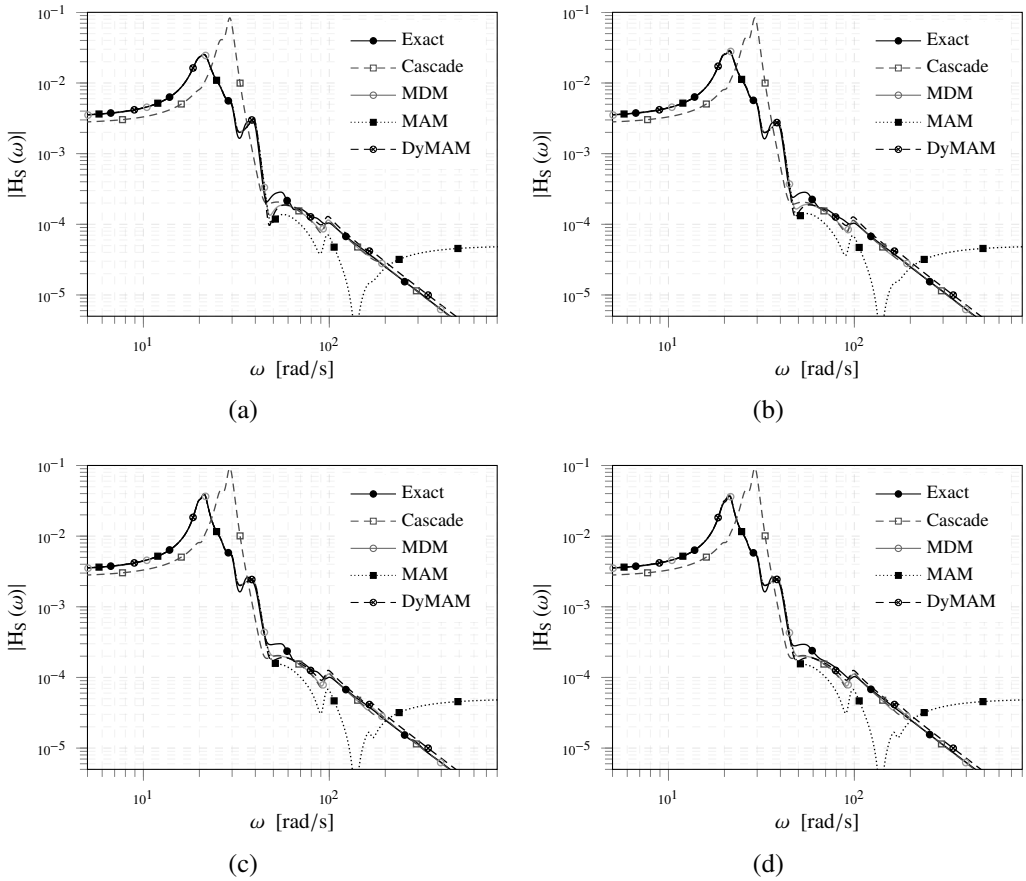


Figure 3: FRF for cascade and MSM with various modal correction methods for single (a) and paired Rayleigh (b), modal (c) and Caughey (d) damping models.

requirement for availability of the ground acceleration time derivatives.

Figure 7 summarises the results of the EDPs under consideration, quantified through each damping model and the three input accelerograms. Although the limited number of earthquake records and the specific features of the case study do not allow drawing general conclusions, the effects of the aforementioned modal correction methods hold true for the remaining damping models and accelerograms. Additionally, it appears that depending on the damping model used, the predicted vibration envelopes will successively reduce in size for modal, Caughey, paired and single Rayleigh damping models, respectively, regardless of the EDP.

It is noted that, while mutual comparison of the various models is permitted throughout the analysis, implementation of a hysteretic damping model in the time domain analysis is currently unattainable for the purpose of numerical validation [23]. Current uncertainties in the characterisation of damping need therefore to be quantified to assess and fully understand the predicted response of vibrating secondary subsystems.

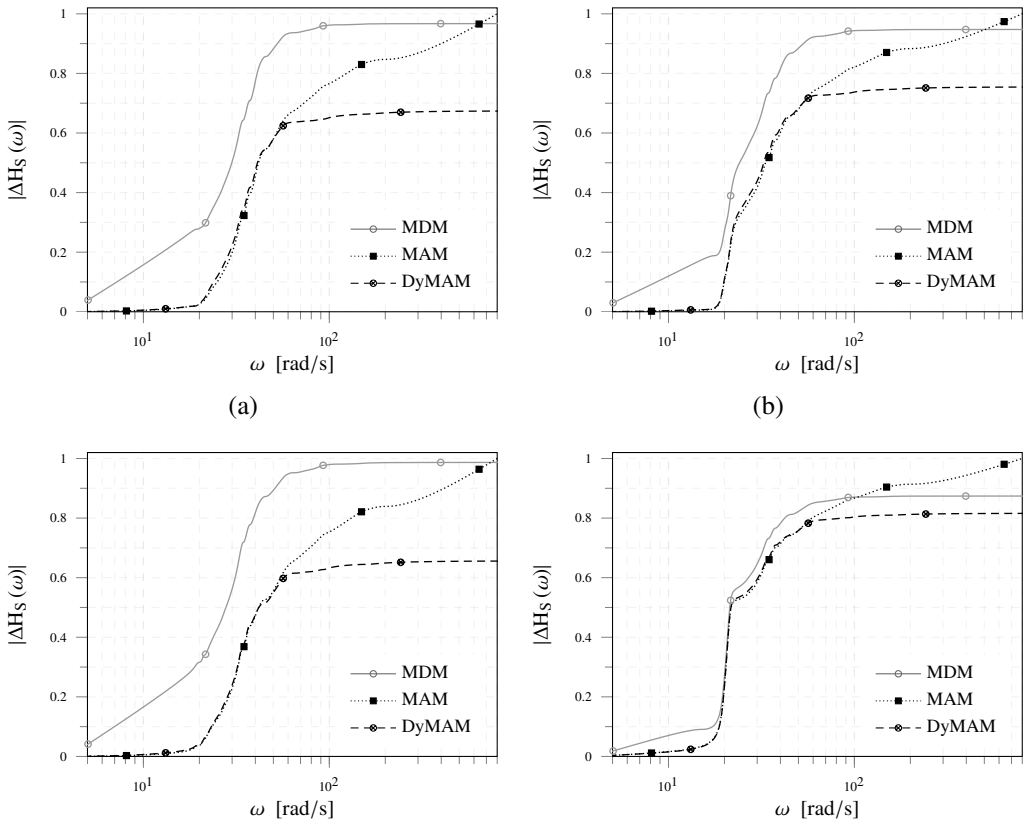


Figure 4: Cumulative inaccuracies of various modal correction methods for single (a), and paired Rayleigh (b), Modal (c) and Caughey (d) damping models.

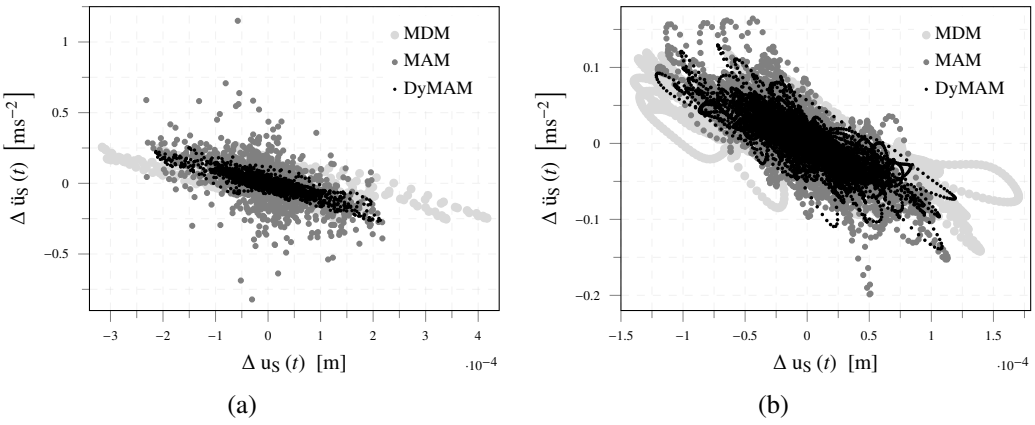


Figure 5: Discrepancies in the phase plane for various modal correction methods for Erzican (a) and Irpinia (b) earthquakes, respectively.

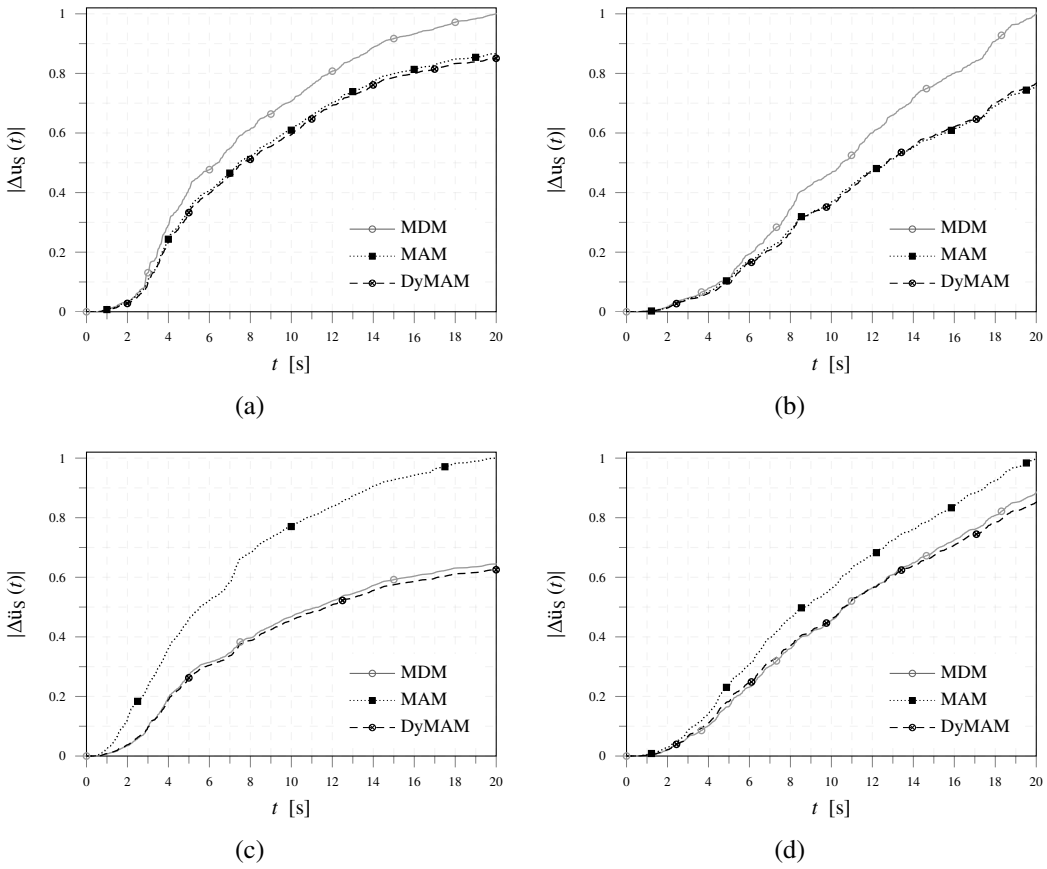


Figure 6: Cumulative inaccuracies in the displacement (a, b) and acceleration (c, d) time histories, for Erzican (left) and Irpinia (right) earthquakes, respectively.

# 4 Conclusions

In this paper, two principal questions related to the seismic response of coupled dynamic systems are addressed. Firstly, the selection of vibrational modes to be retained in analysis is discussed and a modal correction method is proposed, to account for the dynamic contribution of the truncated modes of a secondary subsystem. Secondly, the influence of various approaches to construct the viscous damping matrix of the primary-secondary assembly is investigated and a novel technique based on modal damping superposition, is proposed. Linear dynamic analyses carried out on a staircase system multi-connected to a two-dimensional multi-storey frame, lend themselves the following conclusions:

- The proposed dynamic MAM (DyMAM) is capable of improving the truncation error due to the MDM while it concurrently ameliorates the discrepancy induced in the high-frequency range by the MAM. It is of paramount importance for secondary systems possessing numerous low-frequency modes with negligible mass, where truncation threshold criteria can hardly be applied. Conversely to

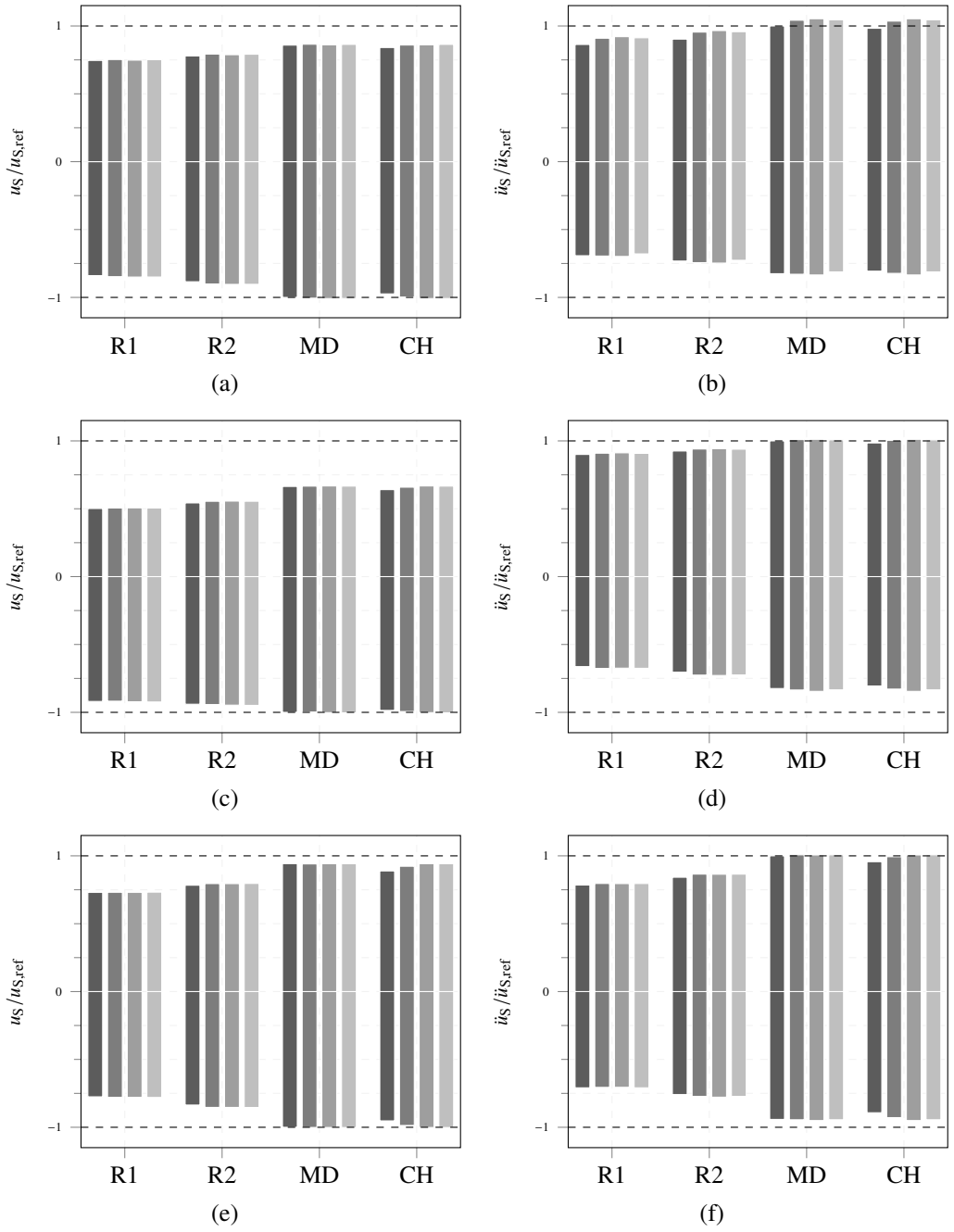


Figure 7: Displacement (left) and acceleration (right) vibration envelopes for the Exact, MDM, MAM and DyMAM cases, from (left to right), respectively, as well as, single and paired Rayleigh (R1, R2), modal (MD) and Caughey (CH) damping models, for Imperial Valley (top), Erzican (middle) and Irpinia (bottom) earhquakes, respectively.

MAM, it has been demonstrated to consistently be applicable on various EDPs, being in accordance with performance-based earthquake engineering principles.

Provided that a good proportion of the mass participating with vibration is considered, its effectiveness will increase with reduced modal information.

- The proposed technique for assembling the damping matrix is shown to be a convenient alternative for modelling the dissipative forces in composite vibrating systems. The predicted vibration envelope was shown to successively reduce in size for modal, Caughey, paired and single Rayleigh damping models, respectively, regardless of the EDP under consideration. An implementation of a hysteretic damping model in the time domain analysis is deemed necessary for the purpose of numerical validation.

Further studies will be devoted to investigate future extension of the proposed formulation to account for uncertainties in the mass, stiffness and damping of both P and S components, as well as the random characteristics of the ground shaking.

# References


[1] S. Taghavi, E. Miranda, "Response assessment of nonstructural building elements", PEER Report 2003/05, University of California Berkeley, 2003.

[2] S. Adham, B. Ballif, "The Borah Peak, Idaho earthquake of October 28, 1983 - Buildings and schools", Earthquake Spectra, 2, 169-182, 1985.

[3] N. Taly, "The Whittier Narrows, California Earthquake of October 1, 1987 - Performance of buildings at California State University, Los Angeles", Earthquake Spectra, 4, 277-317, 1988.

[4] B. Reitherman, T. Sabol, R. Bachman, D. Bellet, R. Bogen, D. Cheu, P. Coleman, J. Denney, M. Durkin, C. Fitch, R. Fleming, W. Gates, B. Goodno, M. Halling and R. Hess, "Nonstructural damage", Earthquake Spectra, 11, 453-514, 1995.

[5] R. Villaverde, "Fundamental concepts of earthquake engineering", Boca Raton, Fla, London, 2009.

[6] G. Muscolino, A. Palmeri, "Seismic analysis of light secondary substructures via an extended response spectrum method", Saxe-Coburg Publications, New Trends in Seismic Design of Structures, 289-321, 2013.

[7] W.C. Hurty, "Vibrations of structural systems by component-mode synthesis", Journal of Engineering Mechanics Division, 86(4), 51-70, 1960.

[8] B. Biondi, G. Muscolino, "Component-mode synthesis method variants in the dynamics of coupled structures", Meccanica, 35(1), 17-38, 2000.

[9] European Committee for Standardisation, "Eurocode 8: Design of structures for earthquake resistance - Part 1 - General rules, seismic actions and rules for buildings", Brussels, 2004.

[10] R.L. Bisplinghoff, H. Ashley, R.L. Halfman "Aeroelasticity", Cambridge, Mass, USA: Addison-Wesley, 1994.

[11] N. Maddox, "On the number of modes necessary for accurate response and resulting forces in dynamic analysis", Journal of Applied Mechanics, 42:516-517, 1975.

[12] O. Hansteen, K. Bell, "On the accuracy of mode superposition analysis in structural dynamics", Earthquake Engineering and Structural Dynamics, 7:405-411, 1979.
[13] R. Cornwell, R. Craig, C. Johnson, "On the application of the mode-acceleration method to structural engineering problems", Earthquake Engineering and Structural Dynamics, 11:679-688, 1983.
[14] T.K. Caughey, M.E.J. O'Kelly, "Classical normal modes in damped linear dynamic systems", Journal of Applied Mechanics, 32:583-588, 1965.
[15] A.K. Chopra "Dynamics of structures: theory and applications to earthquake engineering", Boston: Prentice Hall, 2012.
[16] A. Palmeri, M. Lombardo, "A new modal correction method for linear structures subjected to deterministic and random loadings", Computers and Structures, 89, 844-854, 2011.
[17] S. Kasinos, A. Palmeri and M. Lombardo, "Performance-based seismic analysis of light SDoF secondary substructures", Proc. $12^{th}$ Int. Conf. on Applications of Statistics and Probability in Civil Engineering, 2015.
[18] G. Muscolino, A. Palmeri, "An earthquake response spectrum method for linear light secondary substructures", ISET Journal of Earthquake Technology, Paper No. 482, 44(1), 193-211, 2007.
[19] Computers and Structures, SAP2000, Release 15.2.1, Berkeley, 2007.
[20] The MathWorks, Inc, MATLAB, Release 8.2, Natick, Massachusetts, United States, 2013.
[21] A. Feriani, F. Perotti, "The formation of viscous damping matrices for the dynamic analysis of MDOF systems", Earthquake engineering and structural dynamics, 25, 689-709, 1996.
[22] International Federation for Structural Concrete, "Probabilistic performance-based seismic design", Technical report, bulletin 68, Lausanne, Switzerland, 2012.
[23] G. Muscolino, A. Palmeri, F. Ricciardelli "Time-domain response of linear hysteretic systems to deterministic and random excitations", Earthquake engineering and structural dynamics, 34, 1129-1147, 2005.